


 Cite this: *RSC Adv.*, 2022, **12**, 30404

Microwave-assisted multicomponent synthesis of antiproliferative 2,4-dimethoxy-tetrahydropyrimido[4,5-*b*]quinolin-6(7*H*)-ones†

Subham G. Patel, ^a Aday González-Bakker, ^b Ruturajsinh M. Vala, ^a Paras J. Patel, ^a Adrián Puerta, ^b Apoorva Malik, ^c Rakesh K. Sharma, ^c José M. Padrón ^b and Hitendra M. Patel ^{a*}

In this study, we demonstrate a simple, highly efficient, rapid and convenient series of 2,4-dimethoxy-tetrahydropyrimido[4,5-*b*]quinolin-6(7*H*)-ones **4a–v**. Microwave irradiation facilitates the one-pot multicomponent reaction of different aromatic aldehydes, 6-amino-2,4-dimethoxypyrimidine and dimedone using glacial acetic acid. Metal-free multicomponent synthesis, shorter reaction time, higher product yield, easy product purification without column chromatography and outstanding green credential parameters are the key features of this protocol. We analysed **4a–v** against six human tumour cell lines for antiproliferative activity. **4h**, **4o**, **4q** and **4v** show good antiproliferative activity with a good *in silico* ADMET profile. Furthermore, **4h**, **4o**, **4q** and **4v** also show drug-likeness properties by obeying drug-like filters.

Received 26th July 2022
 Accepted 17th October 2022

DOI: 10.1039/d2ra04669e

rsc.li/rsc-advances

1. Introduction

The worldwide burden of tumours and cancer has been steadily increasing and is expected to continue to rise in the next decades because of population ageing and urban lifestyles.¹ So, the need to develop antitumor agents has also increased in recent times. Previously we reported antiproliferative activity of pyrimidine and quinoline based heterocycles against six human tumour cell lines. In this work, we developed novel pyrimidine and quinoline based heterocycles to develop a new potent antiproliferative agent.^{2,3} Multicomponent reactions (MCRs) facilitated by microwave irradiation are an effective strategy from the perspective of green chemistry.⁴ Microwave irradiation is a powerful tool in heterocyclic chemistry as well as drug discovery.^{4,5} When MW radiation comes into contact with solvent, bubbles develop, grow and then burst, generating hot regions of high temperature and pressure. These hot regions generate enough energy to progress the reaction due to the elevation in number of species. These species produce sufficient kinetic energy to exceed the activation energy barrier.⁶ Microwave irradiation has numerous benefits, such as being

homogeneous and quick heating, having shorter reaction times, higher reaction rates, lower energy consumption and low waste production.^{7,8} As a result, synthesis utilizing MCRs under MW irradiation proceeds effortlessly and in a benign way.

In 2010, pyrimido[4,5-*b*]quinolines (PQs) were reported as a new class of antitumor agents and found PQ **I** as a potent antitumor agent.⁹ Other research groups then worked on PQs and explored more antitumor PQs (**II–III**) (Fig. 1a).^{10,11} Thus, PQs are the best candidate to explore new antitumor agents. Some mechanisms for the anticancer effects of pyrimido[4,5-*b*]quinolines were reported including the inhibition of vascular epithelial growth factor receptor tyrosine kinase,¹² topoisomerases I and Epidermal growth factor receptor.¹³ In other case, pyrimido[4,5-*b*]quinolines showed the anticancer effects through caspase-3 activation. They also inhibited tubulin polymerization, arrested cell cycle at G2/M phase and induced apoptosis.¹⁴ Methoxy group containing heterocycles have more potential of antitumor or anticancer activity. For instance, **II** and **III** of Fig. 1a contain methoxy group in their molecules. Many anticancer drugs like bosutinib,¹⁵ brigatinib,¹⁶ cabazitaxel,¹⁷ erdafitinib,¹⁸ lurbinectedin¹⁹ and trabectedin²⁰ contain methoxy group in their chemical structure. So, here we developed methoxy group containing PQs *i.e.*, 2,4-dimethoxy-tetrahydropyrimido[4,5-*b*]quinolin-6(7*H*)-ones (2,4-dimethoxy-THPQs).

In our previous work, 2,4-dimethoxy-THPQs were synthesised by conventional heating in acetic acid medium.²¹ To improve the protocol, irradiation of microwave was used for acceleration of multicomponent synthesis. Irradiation of microwave was used in the synthesis of heterocycle because it

^aDepartment of Chemistry, Sardar Patel University, Vallabh Vidyanagar, 388120, Gujarat, India. E-mail: hm_patel@spuvm.edu

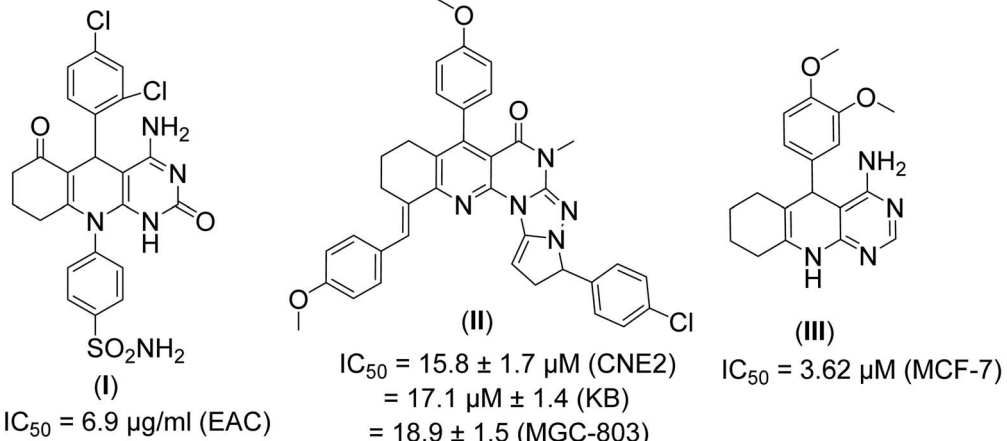
^bBioLab, Instituto Universitario de Bio-Organica Antonio Gonzalez (IUBO-AG), Universidad de La Laguna, La Laguna E-38206, Spain

^cSustainable Materials and Catalysts Research Laboratory (SMCRL), Department of Chemistry, Indian Institute of Technology, Jodhpur, India

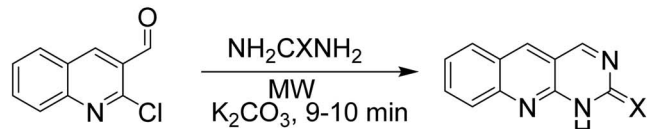
† Electronic supplementary information (ESI) available. CCDC 2157101 and 2149724. For ESI and crystallographic data in CIF or other electronic format see DOI: <https://doi.org/10.1039/d2ra04669e>



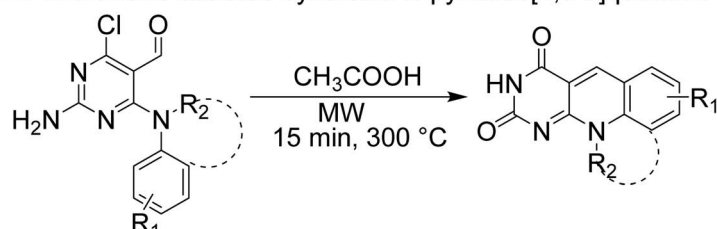
a) Potent antitumour Pyrimido[4,5-b]quinolines



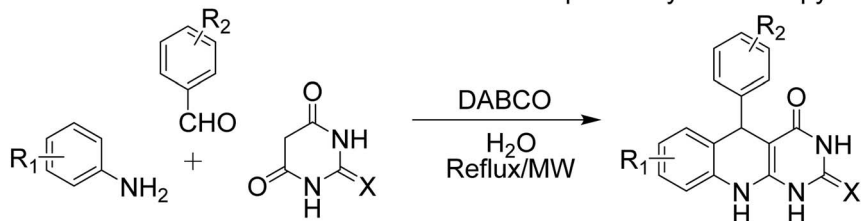
b) Naik's work: Microwave assisted synthesis of pyrimido[4,5-b]quinoline from 2-chloro-3-formylquinoline



c) Quiroga's work: Microwave assisted synthesis of pyrimido[4,5-b]quinoline by cyclization



d) Mosslemin's work: Microwave assisted multicomponent synthesis of pyrimido[4,5-b]quinoline



e) This work:

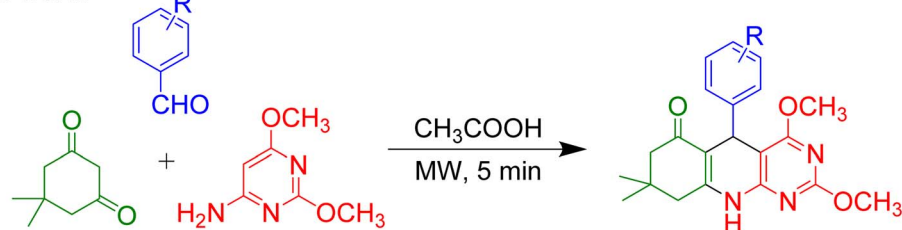


Fig. 1 (a) Representative PQs with antiproliferative activity. (b-d) Reported synthetic strategies to obtain PQs. (e) Synopsis of the synthetic methodology reported in this work.

offers unique advantages. It reduces the time of the reaction and enhances the yield.²² Fig. 1 shows previous work on microwave-assisted synthesis of PQs. The microwave-assisted reaction of 2-chloro-3-formylquinoline with urea/thiourea produced PQs in 9–10 minutes (Fig. 1b).²³ Microwave-assisted cyclisation reaction of 2,4-diamino-6-chloropyrimidine-5-carbaldehydes in the presence of acetic acid produced PQs

(Fig. 1c).²⁴ The microwave-assisted multicomponent reaction of aldehyde, amine and (thio)barbituric acid also produced PQs (Fig. 1d).²⁵ In this work, 2,4-dimethoxy-THPQs were synthesised by microwave-assisted multicomponent reaction of aldehydes, dimedone and 6-amino-2,4-dimethoxypyrimidine in continuation of our work on exploring novel bioactive heterocycles (Fig. 1e).^{26–32} 2,4-dimethoxy-THPQs were then evaluated for *in vitro*

antiproliferative activity against six human tumour cell lines. Furthermore, the most potent 2,4-dimethoxy-THPQs are evaluated by *in silico* ADMET and drug-likeness properties.

2. Results and discussions

2.1. Chemistry

In the above concept, we selected *p*-chlorobenzaldehyde **1a**, 6-amino-2,4-dimethoxypyrimidine **2** and dimedone **3** as model substrates to explore the microwave irradiated multicomponent synthesis of **4a** (Scheme 1). In order to check the effect of the selected solvent and catalyst, we optimised the reaction by different reaction conditions (Table 1). Complete conversion of **1a** into **4a** did not observe in catalyst-free condition with ethanol and water (Table 1, entry 1–3). As discussed earlier, *p*-TSA is the best catalyst for similar reactions. So, we utilised it for optimisation (Table 1, entry 4–7). Best results were observed when glacial acetic acid was used as a solvent. At room temperature, *p*-TSA/AcOH converted **1a** to **4a** in 25 minutes. In comparison, *p*-TSA/AcOH converted **1a** to **4a** in 10 minutes under reflux. Similar results are also observed in the case of glacial acetic acid only (Table 1, entry 8 and 9). So, we decided to proceed with the best-optimised condition (Table 1, entry 9) in which desired product **4a** was obtained in only 10 minutes by glacial acetic acid under reflux.

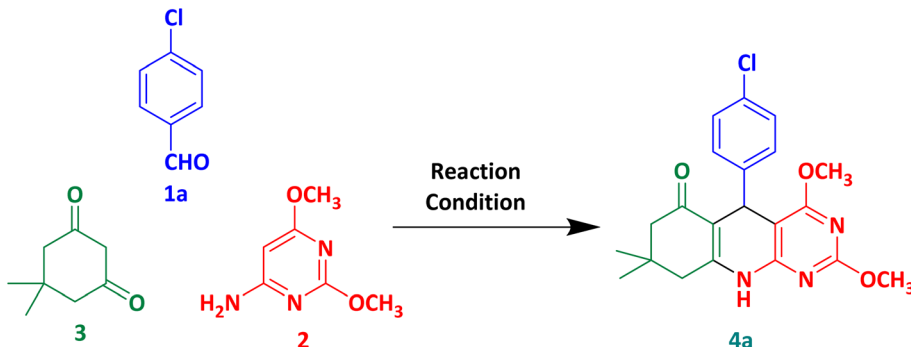
In order to check the effect of microwave irradiation power, we optimised the reaction by applying different microwave irradiation power (Table 2). The best results were obtained by applying 75 W MW with the highest 84% isolated yield in only 5 minutes.

We also carried out a reaction with a similar protocol with conventional heating (Table 1, entry 10). It produced **4a** in 90 minutes by glacial acetic acid under reflux with 73% isolated yield. To evaluate the greenness of the conventional *vs.* microwave synthesis, the green metrics (see ESI† for the definition of

Table 2 Optimization of the power of microwave irradiation for synthesis of **4a**^a

Entry	Power (W)	Time (Min)	Yield ^b (%)
1	200	10	78
2	150	10	82
3	150	5	83
4	100	10	82
5	75	10	80
6	75	5	84
7	50	5	83

^a Reaction condition: 1 mmol *p*-chlorobenzaldehyde **1a**, 1 mmol 6-amino-2,4-dimethoxypyrimidine **2** and 1 mmol dimedone **3**, 3 mL acetic acid, reflux. ^b Isolated yield.



Scheme 1 Three-component synthesis of **4a** from *p*-chlorobenzaldehyde, 6-amino-2,4-dimethoxypyrimidine and dimedone.

Table 1 Optimization of solvent and catalyst for the preparation of compound **4a** under Microwave irradiation^a

Entry	Catalyst	Solvent ^b	Temperature	Time (min)	Conversion relative to aldehyde ^c
1	—	Water	RT	—	—
2	—	Ethanol	RT	—	—
3	—	Ethanol	Reflux	35	Incomplete
4	<i>p</i> -TSA (20 mol%)	Ethanol	Reflux	45	100%
5	<i>p</i> -TSA (20 mol%)	Acetonitrile	Reflux	30	100%
6	<i>p</i> -TSA (20 mol%)	Acetic acid	RT	25	100%
7	<i>p</i> -TSA (20 mol%)	Acetic acid	Reflux	10	100%
8	—	Acetic acid	RT	25	100%
9	—	Acetic acid	Reflux	10	100%
10	—	Acetic acid	Reflux	90	100% ^d

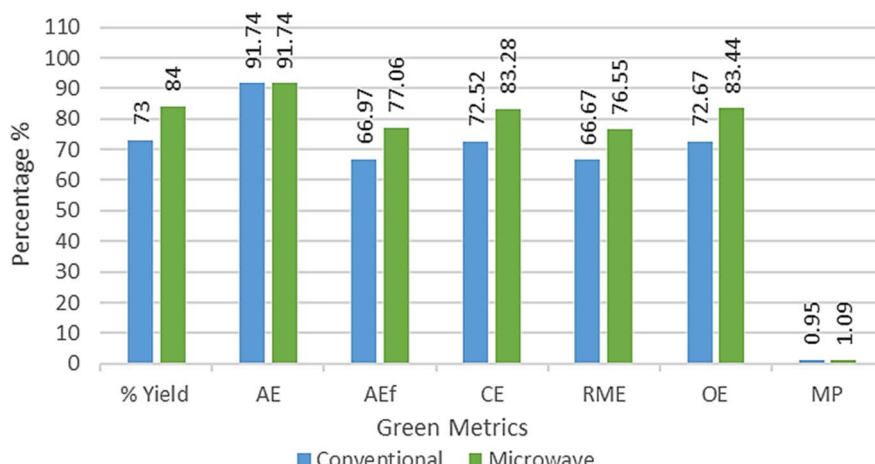
^a Reaction condition: 1 mmol *p*-chlorobenzaldehyde **1a**, 1 mmol 6-amino-2,4-dimethoxypyrimidine **2** and 1 mmol dimedone **3**, 200 W MW. ^b 3 mL solvent. ^c Observed from TLC analysis. ^d Obtained by conventional heating.



Table 3 Green metrics (AE, AEf, CE, RME, OE and MP) analysis for conventional and microwave synthesis of 4a

Method	% Yield ^a	AE	AEf	CE	RME	OE	MP
Conventional	73	91.74	66.97	72.52	66.67	72.67	0.95
Microwave	84	91.74	77.06	83.28	76.55	83.44	1.09

Higher the value, greener the process



^a Isolated yield. Abbreviation: AE: atom economy, AEf: atom efficiency, CE: carbon efficiency, RME: reaction mass efficiency, OE: optimum efficiency, MP: mass productivity.

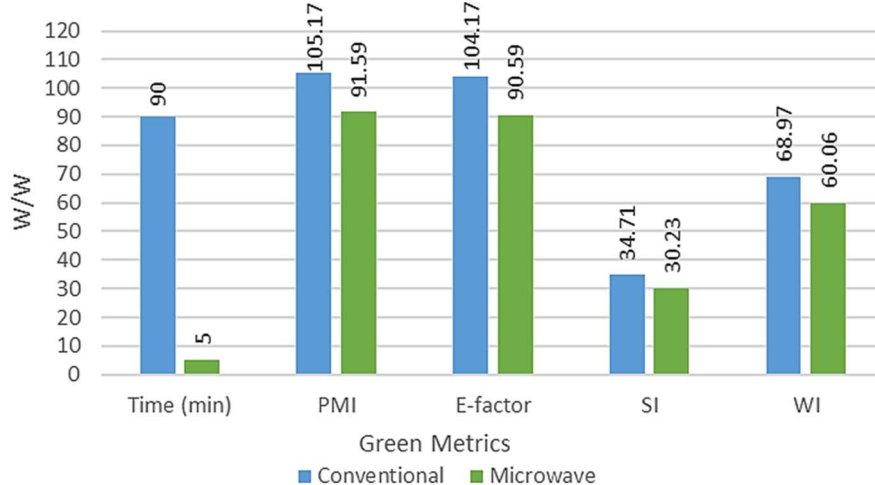
green metrics and detailed calculation process) were conducted and the results are shown in Tables 3 and 4. The AE for both conventional vs. microwave synthesis is 91.74% due to the same reactants. AEf, CE, RME, OE and MP of microwave is higher

than the conventional method. Whereas PMI, E-factor, SI and WI of microwave is lower than the conventional method. So, from both ways, the microwave process is greener than the

Table 4 Green metrics (PMI, E-factor, SI and WI) analysis for conventional and microwave synthesis of 4a^a

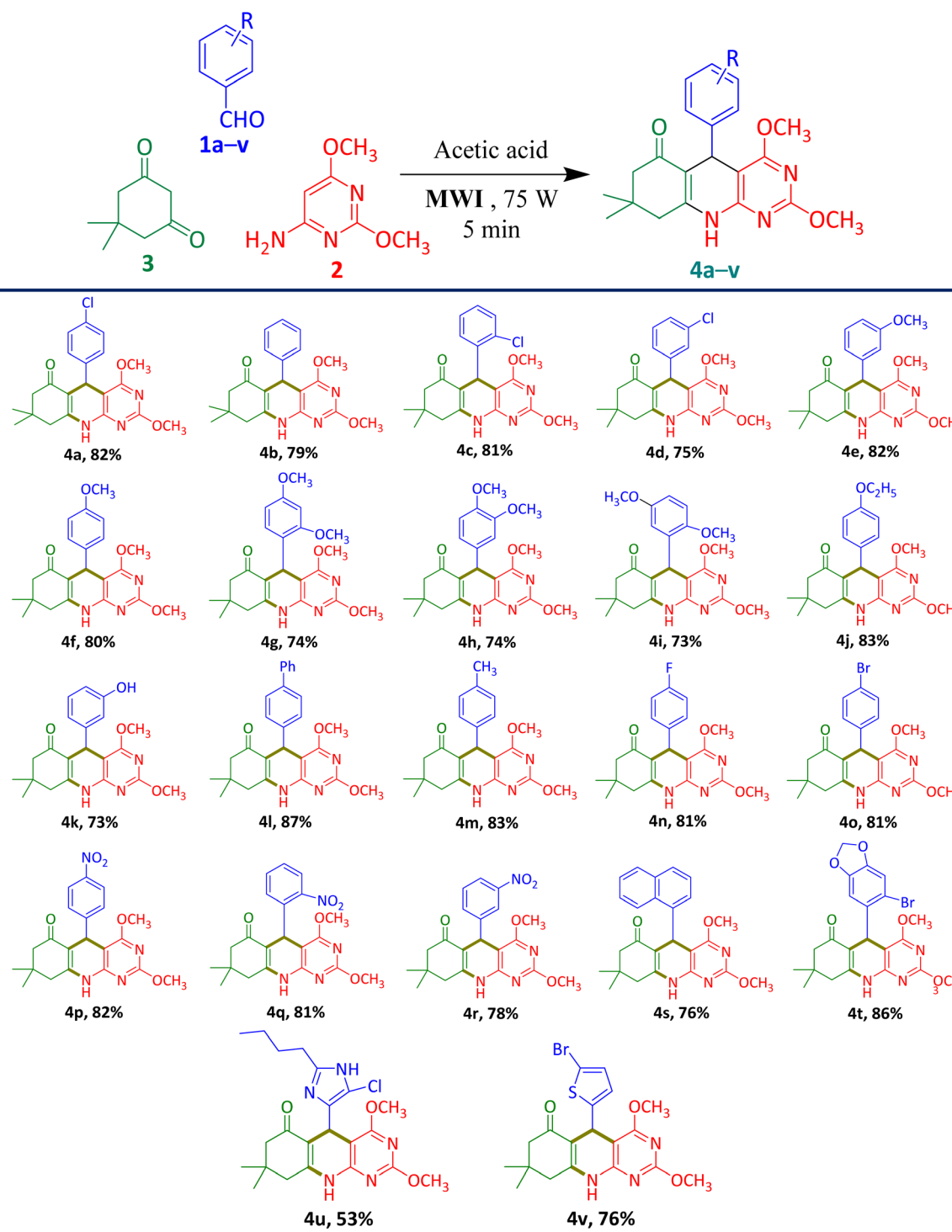
Method	Time (min)	PMI	E-factor	SI	WI
Conventional	90	105.17	104.17	34.71	68.97
Microwave	5	91.59	90.59	30.23	60.06

Lower the value, greener the process



^a PMI: process mass intensity, E-factor: environmental factor, SI: solvent intensity and WI: water intensity.



Table 5 Substrate scope of the synthesis of 2,4-dimethoxy-THPQs 4a–v^a

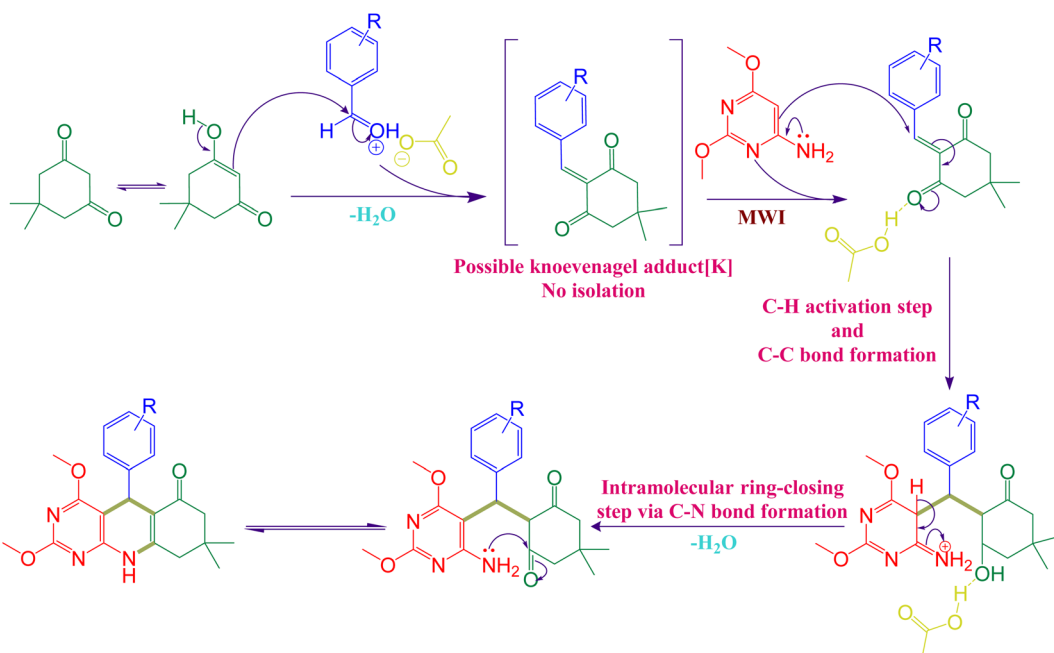
^a Reaction condition: 1 mmol aldehyde 1, 1 mmol 6-amino-2,4-dimethoxypyrimidine 2 and 1 mmol dimedone 3, 3 mL AcOH, 75 W MW, Reflux. Isolated yields are mentioned with the product.

conventional method for the reaction of model substrates 1a, 2 and 3.

With the best optimal reaction condition in hand, we then explore the substrate scope of this 2,4-dimethoxy-THPQ derivative using different substituted aromatic/heteroaromatic

aldehyde 1a–v with dimedone 2 and 6-amino-2,4-dimethoxypyrimidine 3. Under this optimal reaction conditions, reaction performed smoothly with both electron-releasing and electron-withdrawing substituted aldehydes and give excellent yield up to 87%.





Scheme 2 A plausible reaction root for the formation of 2,4-dimethoxy-THPQs.

Using this green protocol, we synthesize twenty-two 2,4-dimethoxy-THPQs **4a–v** from variety of substrate (Table 5). In primary investigation, formation of desired product was confirmed by TLC analyses using mixture of 30% ethyl acetate and 70% *n*-hexane. The desired product was obtained with minor impurities, which were easily removed by washing of ice-cold diethyl ether. The derivatives **4p–t** were purified by washing with ice-cold aqueous methanol. The derivative **4u** was soluble in water when reaction mixture poured into water, after 20 minutes pure solid product was formed which was isolated by filtration.

The structure of all the synthesized compound were characterised *via*. ¹H NMR, ¹³C NMR and either HRMS or LCMS analysis. Furthermore, we developed a single crystal of product **4f** and **4o** and it was studied using single-crystal X-ray diffraction (SCXRD). The structure of **4f** and **4o** were fully confirmed by results of the analysis. The single-crystal XRD data of **4f** shows that it was crystallises in monoclinic crystal system, space group *C*2/*c* with unit cell dimension *a* = 17.3963(6) Å, *b* = 22.485(1) Å, *c* = 14.0877(9) Å, α = 90°, β = 127.7461(13)°, γ = 90°, *V* = 4357.3(4) Å³, *Z* = 8, density = 1.206 g cm⁻³ and linear absorption coefficient 0.084 mm⁻¹. The product **4o** crystallises in triclinic crystal system, space group *P*-1 with unit cell dimension *a* = 6.0680(2) Å, *b* = 13.0347(5) Å, *c* = 13.5866(5) Å, α = 103.302(3)°, β = 95.6327(18)°, γ = 103.2902(19)°, *V* = 1004.76(7) Å³, *Z* = 2, density = 1.469 g cm⁻³ and linear absorption coefficient 2.072 mm⁻¹. XRD data were deposited online to Cambridge Crystallographic Data Centre (CCDC). CCDC deposition number 2157101 and 2149724 contain the ESI crystallographic data for this paper.

Herein, we proposed plausible reaction root based on the literature reports,^{33,34} (Scheme 2). Firstly, Knoevenagel

condensation was carried out in between aromatic aldehyde and dimedone in presence of acetic acid under microwave irradiation and resulting in the formation of possible Knoevenagel adduct (K) by elimination of first water molecule. In next step, 6-amino-2,4-dimethoxy aniline readily undergoes nucleophilic attack on this Knoevenagel adduct (K) and produce an imine derivative. In the final step, this imine derivative undergoes intramolecular ring-closing step *via* C–N bond formation by elimination of second water molecule in presence of acetic acid and furnished the final product.

2.2. Antiproliferative activity

The antiproliferative activity of 2,4-dimethoxy-THPQs was **4a–v** studied in a panel of six human solid tumour cell lines. From the initial set of compounds **4a–v** derivatives, **4c–e**, **4l** and **4s** were not tested due to their poor solubility under the experimental conditions. The results reported as 50% growth inhibition (GI₅₀) are shown in Table 6. The results are best compared in the GI₅₀ range plot (Fig. 2). The data from the GI₅₀ range plot reveals that most of the compounds have similar activity across the cell line panel. The most active compounds of the series (**4h**, **4o**, **4q** and **4v**) displayed GI₅₀ values at comparable range that the one displayed by CDDP. From the results, it is not possible to obtain a clear structure–activity relationship (SAR). For instance, compound **4h** holds an electron-donating group (OMe) at *para* position and **4o** has an electron-withdrawing group (Br), whilst **4q** bears a nitro group in *ortho* position.

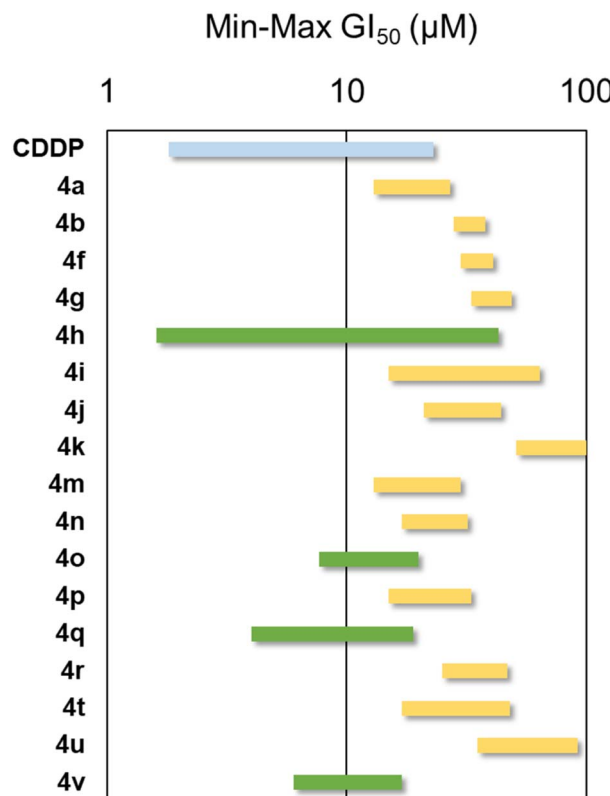
2.3. ADMET prediction

Potent antiproliferative 2,4-dimethoxy-THPQs **4h**, **4o**, **4q** and **4v** were evaluated for *in silico* ADMET prediction which is important drug profiling for novel drug discovery.³⁵ Various filters



Table 6 Antiproliferative activity (GI_{50} , μM) against human solid tumour cell lines

Compound	A549 (lung)	HBL-100 (breast)	HeLa (cervix)	SW1573 (lung)	T-47D (breast)	WiDr (colon)
4a	13 \pm 5.1	24 \pm 7.9	17 \pm 5.8	27 \pm 0.71	26 \pm 6.5	17 \pm 1.6
4b	29 \pm 4.2	38 \pm 8.1	28 \pm 4.8	37 \pm 7.5	33 \pm 5.7	31 \pm 9.1
4f	30 \pm 4.5	41 \pm 8.6	33 \pm 0.87	38 \pm 0.95	32 \pm 1.7	39 \pm 6.5
4g	38 \pm 1.6	41 \pm 12	34 \pm 3.4	46 \pm 1.4	33 \pm 10	49 \pm 12
4h	37 \pm 4.8	1.6 \pm 0.47	27 \pm 1.4	43 \pm 6.5	23 \pm 3.1	42 \pm 8.4
4i	45 \pm 9.7	64 \pm 31	40 \pm 14	15 \pm 6.0	37 \pm 4.7	44 \pm 7.5
4j	28 \pm 5.5	35 \pm 7.8	34 \pm 11	21 \pm 7.0	39 \pm 16	44 \pm 21
4k	51 \pm 7.7	81 \pm 17	>100	60 \pm 2.6	83 \pm 29	83 \pm 18
4m	24 \pm 1.3	29 \pm 13	13 \pm 6.1	30 \pm 0.87	21 \pm 7.1	30 \pm 3.6
4n	19 \pm 3.5	24 \pm 3.7	27 \pm 4.6	32 \pm 5.4	17 \pm 1.6	26 \pm 1.1
4o	7.7 \pm 2.4	19 \pm 7.9	8.3 \pm 1.1	20 \pm 1.3	16 \pm 3.2	12 \pm 5.8
4p	23 \pm 6.1	33 \pm 4.2	15 \pm 0.4	21 \pm 8.6	27 \pm 1.9	31 \pm 4.6
4q	12 \pm 4.7	10 \pm 3.2	4.0 \pm 0.98	8.0 \pm 0.45	10 \pm 2.8	19 \pm 0.88
4r	25 \pm 3.4	35 \pm 5.1	30 \pm 8.9	47 \pm 15	32 \pm 0.14	36 \pm 1.9
4t	30 \pm 1.9	37 \pm 15	25 \pm 11	17 \pm 0.77	48 \pm 12	35 \pm 0.4
4u	47 \pm 15	88 \pm 21	71 \pm 26	35 \pm 1.7	92 \pm 13	80 \pm 29
4v	9.5 \pm 0.15	17 \pm 7.9	11 \pm 3.4	6.0 \pm 0.10	16 \pm 6.3	14 \pm 4.1
CDDP	4.9 \pm 0.2	1.9 \pm 0.2	1.8 \pm 0.5	2.7 \pm 0.4	17 \pm 3.3	23 \pm 4.3

Fig. 2 GI_{50} range plot against human solid tumour cell lines. Cisplatin (CDDP) was used as reference anticancer drug (blue bar). Green bars indicate the most active compounds.

such as Lipinski filter, Ghose filter, Veber filter, Egan filter and Muegge filter are help to predict drug likeness based on their physicochemical properties. **4h**, **4o**, **4q** and **4v** were evaluated for their ADMET properties with the help of the online web server SwissADME (<http://www.swissadme.ch>). Calculated physicochemical properties of are summarised in Table 7.

Bioavailability radar plot of 2,4-dimethoxy-THPQs **4h**, **4o**, **4q** and **4v** show in Fig. 3 display that all four 2,4-dimethoxy-THPQs have drug like radar plot. Calculated bioavailability score found as 0.55 for all 2,4-dimethoxy-THPQs. To predict the gastrointestinal absorption and blood–brain barrier permeability of 2,4-dimethoxy-THPQs **4h**, **4o**, **4q** and **4v**, BOILED-Egg delineation was used. BOILED-Egg delineation of these 2,4-dimethoxy-THPQs is illustrated in Fig. 4. “The white region is the physicochemical space of molecules with highest probability of being absorbed by the gastrointestinal tract, and the yellow region (yolk) is the physicochemical space of molecules with highest probability to permeate to the brain”.³⁶ **4h**, **4q** and **4v** show high gastrointestinal absorbance, and they have no blood–brain permeability. While **4o** show blood–brain permeability. Red dots for **4o** and **4v** denoted that they are not P-gp substrates while blue dots for **4h** and **4q** denoted that they are P-gp substrates.

3. Experimental section

3.1. General methods

For synthesis, all chemical reagents were purchased from the TCI, Sigma-Aldrich and Sisco Research Laboratories Pvt. Ltd and used without further purification. The microwave-assisted reactions were performed in a “SINEO UWAVE-1000 Microwave, UV, US Synthesis Extraction Reactor”. The progress of all chemical reactions was monitored by thin-layer chromatography (TLC, on aluminium plates pre-coated with F254 silica gel 60). Melting points of all solid compounds were determined by the open capillary tube method and are uncorrected. High-resolution mass spectra (HRMS) were acquired using Agilent technologies model G6564 QTOF. The samples were ionized in positive ion mode using a MALDI or ESI ionization sources. The LCMS analysis was collected on an MS-Agilent 6120 quadrupole. Nuclear magnetic resonance spectra (^1H NMR & ^{13}C NMR) were recorded on a Bruker 500 MHz WB FT-NMR spectrometer having

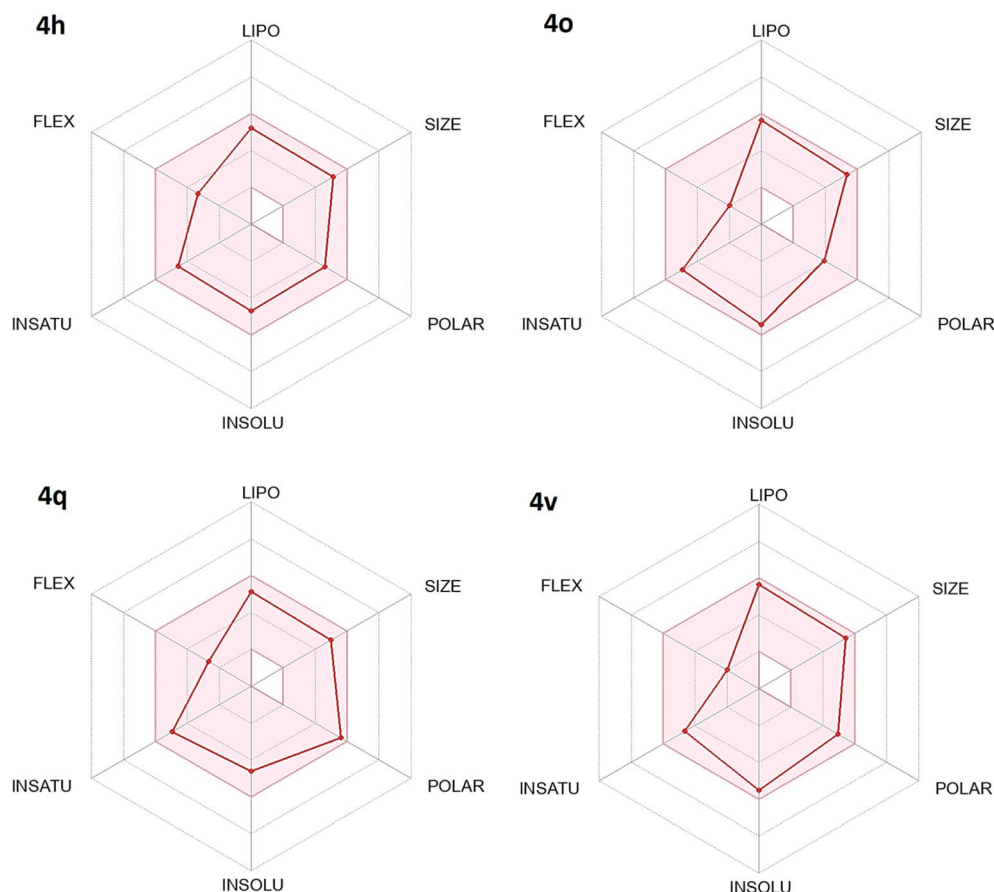


Table 7 Physicochemical properties of **4h**, **4o**, **4q** and **4v** with various filters for drug-likeness^a

Comp.	MW	RB	HBA	HBD	MR	TPSA	X log P	W log P	M log P	NR	NC	NH	Atom
4h	425.48	5	7	1	118.58	91.8	3.62	3.14	1.97	4	23	8	58
4o	444.32	3	5	1	113.3	73.34	4.36	3.89	3.18	4	21	7	50
4q	410.42	4	7	1	114.42	119.16	3.5	3.03	1.7	4	21	9	52
4v	450.35	3	5	1	111.17	101.58	4.41	3.95	2.78	4	19	8	47

Lipinski filter	Ghose filter	Veber filter	Egan filter	Muegge filter
$MW \leq 500$	$160 \leq MW \leq 480$	$RB \leq 10$	$WlogP \leq 5.88$	$200 \leq MW \leq 600$
$M log P \leq 4.15$	$-0.4 \leq W log P \leq 5.6$	$TPSA \leq 140$	$TPSA \leq 131.6$	$-2 X log P \leq 5; TPSA \leq 150$
$HBA \leq 10$	$40 \leq MR \leq 130$			$NR \leq 7; NC > 4; NH > 1; RB \leq 15; HBA \leq 10; HBD \leq 5$
$HBD \leq 5$	$20 \leq atoms \leq 70$			

^a Abbreviation: MW: molecular weight; RB: rotational bond; HBA: H-bond acceptor; HBD: H-Bond Donor; MR: Molecular Refractivity; TPSA: Topological Polar Surface Area; NR: No. of ring; NC: No. of Carbon; NH: No. of Heteroatoms.

Fig. 3 Bioavailability radar of 2,4-dimethoxy-THPQs **4h**, **4o**, **4q** and **4v**.

proton noise decoupling mode with a standard 5 mm probe using $CDCl_3$ and $DMSO-d_6$ solution. Abbreviations are used for the 1H NMR signal are as follows: s = singlet, d = doublet, t = triplet, q = quartet dd = double doublet, td = triple doublet, m = multiplet. The chemical shifts are reported in parts per million and coupling constants (γ) are provided in Hertz.

3.2. General procedure for synthesis of 2,4-dimethoxy-THPQs **4a–v**

A mixture of aromatic aldehydes (**1**, 1 mmol), 6-amino-2,4-dimethoxy pyrimidine (**2**, 1 mmol), dimedone (**3**, 1 mmol) and acetic acid (3 mL) were charged into a microwave vessel. The



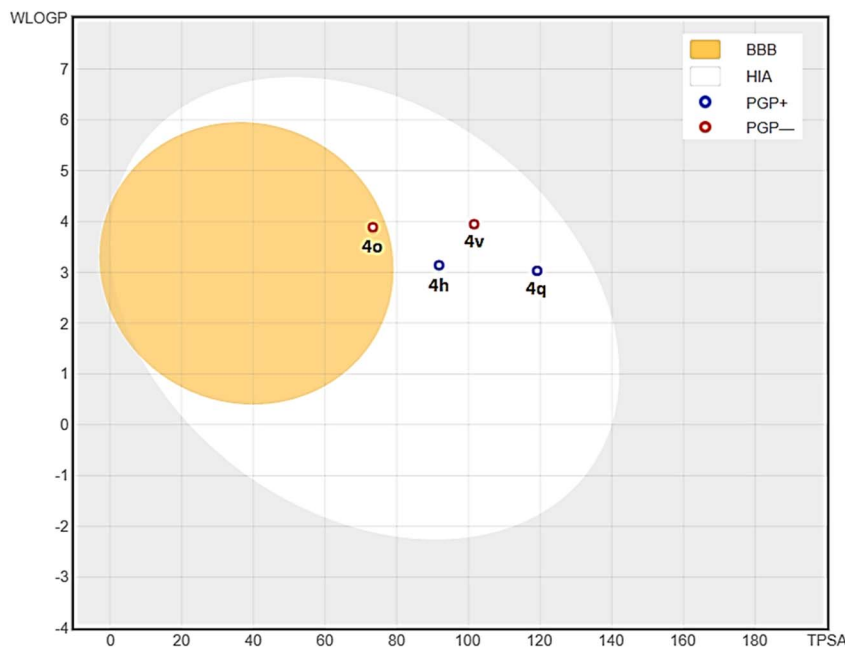


Fig. 4 BOILED-Egg model of 2,4-dimethoxy-THPQs **4h**, **4o**, **4q** and **4v**.

reaction mixture was heated at 110 °C (75 W) by MW irradiation for 5 min. The reaction progress was monitored on TLC using *n*-hexane : ethyl acetate (70 : 30, v/v) as mobile phase. After complete consumption of starting material, the reaction mixture was cooled to room temperature and poured into 20 mL cold water. The obtained crude product was filtered and dried in an oven. Further purification, the crude product was stirred in 5 mL ice-cold diethyl ether or methanol as mentioned in results and discussion to obtain pure product. The products **4f** and **4o** were crystallised by a slow evaporation method using a mixture of 20 mL dichloromethane and 3 mL methanol.

3.2.1. 5-(4-Chlorophenyl)-2,4-dimethoxy-8,8-dimethyl-5,8,9,10-tetrahydropyrimido[4,5-*b*]quinolin-6(7*H*)-one (4a). White solid, mp. 208–210 °C; ¹H-NMR (500 MHz, CDCl₃) (δ, ppm): 8.46 (s, 1H, NH), 7.26 (d, *J* = 8.5 Hz, 2H, ArH), 7.17 (d, *J* = 8.5 Hz, 2H, ArH), 5.17 (s, 1H, CH), 3.92 (s, 3H, OCH₃), 3.89 (s, 3H, OCH₃), 2.46 (s, 2H, CH₂), 2.26 (d, *J* = 16 Hz, 1H, CH₂), 2.19 (d, *J* = 16 Hz, 1H, CH₂), 1.09 (s, 3H, CH₃), 1.00 (s, 3H, CH₃); ¹³C-NMR (125 MHz, CDCl₃) (δ, ppm): 195.0, 168.8, 163.4, 156.5, 150.3, 144.5, 131.8, 129.3, 128.1, 111.6, 95.9, 54.4, 54.1, 50.6, 41.2, 33.8, 32.6, 29.4, 27.3; HRMS(ESI-MS) 400.0996 [M + H]⁺.

3.2.2. 2,4-Dimethoxy-8,8-dimethyl-5-phenyl-5,8,9,10-tetrahydropyrimido[4,5-*b*]quinolin-6(7*H*)-one (4b). White solid, mp 244–246 °C; ¹H-NMR (500 MHz, CDCl₃) (δ, ppm): 8.05 (s, 1H, NH), 7.31 (d, *J* = 7.5 Hz, 2H, ArH), 7.20 (t, *J* = 7.5 Hz, 2H, ArH), 7.11 (t, *J* = 7.25 Hz, 1H, ArH), 5.21 (s, 1H, CH), 3.91 (s, 3H, OCH₃), 3.89 (s, 3H, OCH₃), 2.45 (s, 2H, CH₂), 2.26 (d, *J* = 16.5 Hz, 1H, CH₂), 2.19 (d, *J* = 16 Hz, 1H, CH₂), 1.09 (s, 3H, CH₃), 1.01 (s, 3H, CH₃); ¹³C-NMR (125 MHz, CDCl₃) (δ, ppm): 195.0, 168.8, 163.3, 156.5, 149.9, 145.9, 128.0, 127.9, 126.2, 112.1, 96.3, 54.4, 54.1, 50.7, 41.3, 34.2, 32.6, 29.4, 27.3; MS(MM-ES + APCI) 364.20 [M – H]⁻.

3.2.3. 5-(2-Chlorophenyl)-2,4-dimethoxy-8,8-dimethyl-5,8,9,10-tetrahydropyrimido[4,5-*b*]quinolin-6(7*H*)-one (4c). White solid, mp 306–308 °C; ¹H-NMR (500 MHz, CDCl₃) (δ, ppm): 7.43 (s, 1H, NH), 7.36 (dd, *J* = 8 Hz, 1H, ArH), 7.25 (dd, *J* = 8 Hz, 1H, ArH), 7.11 (td, *J* = 7 Hz, 1H, ArH), 7.04 (td, *J* = 8 Hz, 1H, ArH), 5.51 (s, 1H, CH), 3.90 (s, 3H, OCH₃), 3.83 (s, 3H, OCH₃), 2.45–2.35 (m, 2H, CH₂), 2.23 (d, *J* = 16.5 Hz, 1H, CH₂), 2.15 (d, *J* = 16.5 Hz, 1H, CH₂), 1.09 (s, 3H, CH₃), 1.02 (s, 3H, CH₃); ¹³C-NMR (125 MHz, CDCl₃) (δ, ppm): 194.8, 169.0, 163.5, 156.1, 149.8, 142.8, 133.3, 131.7, 129.7, 127.4, 126.3, 54.5, 53.9, 50.5, 41.5, 33.7, 32.5, 29.3, 27.4; HRMS(+ESI) 400.1422 [M + H]⁺.

3.2.4. 5-(3-Chlorophenyl)-2,4-dimethoxy-8,8-dimethyl-5,8,9,10-tetrahydropyrimido[4,5-*b*]quinolin-6(7*H*)-one (4d). White solid, mp 240–242 °C; ¹H-NMR (500 MHz, CDCl₃) (δ, ppm): 7.56 (s, 1H, NH), 7.23–7.21 (m, 2H, ArH), 7.15–7.09 (m, 2H, ArH), 5.16 (s, 1H, CH), 3.92 (s, 3H, OCH₃), 3.90 (s, 3H, OCH₃), 2.44 (s, 2H, CH₂), 2.26 (d, *J* = 16 Hz, 1H, CH₂), 2.20 (d, *J* = 16.5 Hz, 1H, CH₂), 1.10 (s, 3H, CH₃), 1.02 (s, 3H, CH₃); ¹³C-NMR (125 MHz, CDCl₃) (δ, ppm): 194.8, 168.9, 163.5, 156.0, 149.7, 147.7, 133.9, 129.2, 127.9, 126.5, 126.3, 111.6, 95.6, 54.7, 54.2, 50.6, 41.4, 34.1, 32.7, 29.2, 27.4; MS(MM-ES + APCI) 398.20 [M – H]⁻.

3.2.5. 2,4-Dimethoxy-5-(3-methoxyphenyl)-8,8-dimethyl-5,8,9,10-tetrahydropyrimido[4,5-*b*]quinolin-6(7*H*)-one (4e). White solid, mp 224–226 °C; ¹H-NMR (500 MHz, CDCl₃) (δ, ppm): 7.18 (s, 1H, NH), 7.13–6.65 (m, 4H, ArH), 5.18 (s, 1H, CH), 3.90 (s, 3H, OCH₃), 3.89 (s, 3H, OCH₃), 3.75 (s, 3H, OCH₃), 2.44 (d, *J* = 16.5 Hz, 1H, CH₂), 2.39 (d, *J* = 17 Hz, 1H, CH₂), 2.25 (d, *J* = 16.5 Hz, 1H, CH₂), 2.21 (d, *J* = 16.5 Hz, 1H, CH₂), 1.09 (s, 3H, CH₃), 1.02 (s, 3H, CH₃); ¹³C-NMR (125 MHz, CDCl₃) (δ, ppm): 194.9, 168.8, 163.3, 159.4, 156.1, 149.4, 147.3, 128.9, 120.3, 113.9, 112.1, 111.4, 96.0, 55.1, 54.5, 54.1, 50.6, 41.5, 34.1, 32.7, 29.3, 27.4; MS(MM-ES + APCI) 394.20 [M – H]⁺.



3.2.6. 2,4-Dimethoxy-5-(4-methoxyphenyl)-8,8-dimethyl-5,8,9,10-tetrahydropyrimido[4,5-*b*]quinolin-6(7*H*)-one (4f). White solid, mp 198–200 °C; ¹H-NMR (500 MHz, CDCl₃) (δ , ppm): 8.60 (s, 1H, NH), 7.23 (d, J = 8.5 Hz, 2H, ArH), 6.74 (d, J = 8.5 Hz, 2H, ArH), 5.16 (s, 1H, CH), 3.91 (s, 3H, OCH₃), 3.90 (s, 3H, OCH₃), 3.73 (s, 3H, OCH₃), 2.46–2.45 (m, 2H, CH₂), 2.27–2.18 (m, 2H, CH₂), 1.08 (s, 3H, CH₃), 1.01 (s, 3H, CH₃); ¹³C-NMR (125 MHz, CDCl₃) (δ , ppm): 195.2, 168.7, 163.1, 157.9, 156.5, 150.2, 138.5, 129.3, 128.8, 113.5, 113.4, 112.0, 96.5, 55.1, 54.3, 54.0, 50.7, 41.1, 33.2, 32.5, 29.4, 27.3; MS(MM-ES + APCI) 394.20 [M – H]⁺.

3.2.7. 5-(2,4-dimethoxyphenyl)-2,4-dimethoxy-8,8-dimethyl-5,8,9,10-tetrahydropyrimido[4,5-*b*]quinolin-6(7*H*)-one (4g). White solid, mp 138–140 °C; ¹H-NMR (500 MHz, CDCl₃) (δ , ppm): 8.33 (s, 1H, NH), 7.30 (d, J = 8.5 Hz, 1H, ArH), 6.39 (dd, J = 8.5 Hz, 1H, ArH), 6.35 (d, J = 2 Hz, 1H, ArH), 5.24 (s, 1H, CH), 3.89 (s, 3H, OCH₃), 3.85 (s, 3H, OCH₃), 3.75 (s, 3H, OCH₃), 3.71 (s, 3H, OCH₃), 2.42 (d, J = 17 Hz, 1H, CH₂), 2.35 (d, J = 16.5 Hz, 1H, CH₂), 2.21 (d, J = 16.5 Hz, 1H, CH₂), 2.13 (d, J = 16.5 Hz, 1H, CH₂), 1.07 (s, 3H, CH₃), 0.97 (s, 3H, CH₃); ¹³C-NMR (125 MHz, CDCl₃) (δ , ppm): 195.1, 168.6, 162.9, 159.2, 158.5, 156.9, 150.3, 131.6, 126.0, 110.5, 103.7, 98.6, 95.7, 55.2, 55.2, 54.3, 53.9, 50.7, 41.3, 32.5, 31.5, 29.6, 26.7; HRMS(+ESI) 426.2021 [M + H]⁺.

3.2.8. 5-(3,4-dimethoxyphenyl)-2,4-dimethoxy-8,8-dimethyl-5,8,9,10-tetrahydropyrimido[4,5-*b*]quinolin-6(7*H*)-one (4h). White solid, mp 208–210 °C; ¹H-NMR (500 MHz, CDCl₃) (δ , ppm): 8.46 (s, 1H, NH), 6.97–6.70 (m, 3H, ArH), 5.17 (s, 1H, CH), 3.921 (s, 3H, OCH₃), 3.916 (s, 3H, OCH₃), 3.84 (s, 3H, OCH₃), 3.80 (s, 3H, OCH₃), 2.47 (s, 2H, CH₂), 2.27 (d, J = 16.5 Hz, 1H, CH₂), 2.22 (d, J = 16.5 Hz, 1H, CH₂), 1.09 (s, 3H, CH₃), 1.03 (s, 3H, CH₃); ¹³C-NMR (125 MHz, CDCl₃) (δ , ppm): 195.2, 168.8, 163.1, 156.5, 150.1, 148.4, 147.4, 138.9, 119.5, 112.0, 111.7, 110.8, 96.4, 55.8, 55.7, 54.4, 54.1, 50.6, 41.2, 33.6, 32.5, 29.6, 27.2; HRMS(+ESI) 426.2026 [M + H]⁺.

3.2.9. 5-(2,5-dimethoxyphenyl)-2,4-dimethoxy-8,8-dimethyl-5,8,9,10-tetrahydropyrimido[4,5-*b*]quinolin-6(7*H*)-one (4i). White solid, mp 206–208 °C; ¹H-NMR (500 MHz, CDCl₃) (δ , ppm): 7.26, 7.21 (s, 2H, NH + CDCl₃), 6.95 (d, J = 3 Hz 1H, ArH), 6.71 (d, J = 9 Hz, 1H, ArH), 6.65–6.63 (m, H, ArH), 5.28 (s, 1H, CH), 3.89 (s, 3H, OCH₃), 3.83 (s, 3H, OCH₃), 3.75 (s, 3H, OCH₃), 3.71 (s, 3H, OCH₃), 2.42 (d, J = 17 Hz, 1H, CH₂), 2.30 (d, J = 17 Hz, 1H, CH₂), 2.21 (d, J = 16.5 Hz, 1H, CH₂), 2.14 (d, J = 16.5 Hz, 1H, CH₂), 1.08 (s, 3H, CH₃), 0.99 (s, 3H, CH₃); ¹³C-NMR (125 MHz, CDCl₃) (δ , ppm): 194.8, 168.7, 163.1, 153.1, 152.1, 134.4, 117.2, 112.0, 111.9, 110.7, 95.4, 56.2, 55.6, 54.4, 54.0, 50.6, 41.59, 32.55, 32.0, 29.4, 27.0; HRMS(+ESI) 426.2020 [M + H]⁺.

3.2.10. 5-(4-ethoxyphenyl)-2,4-dimethoxy-8,8-dimethyl-5,8,9,10-tetrahydropyrimido[4,5-*b*]quinolin-6(7*H*)-one (4j). White solid, mp 192–194 °C; ¹H-NMR (500 MHz, CDCl₃) (δ , ppm): 8.49 (s, 1H, NH), 7.21 (d, J = 9 Hz, 2H, ArH), 6.73 (d, J = 8.5 Hz, 2H, ArH), 5.15 (s, 1H, CH), 3.97–3.92 (m, 2H, CH₂), 3.91 (s, 3H, OCH₃), 3.89 (s, 3H, OCH₃), 2.46–2.44 (m, 2H, CH₂), 2.27–2.18 (m, 2H, CH₂), 1.35 (t, J = 7 Hz, 3H, CH₃), 1.08 (s, 3H, CH₃), 1.00 (s, 3H, CH₃); ¹³C-NMR (125 MHz, CDCl₃) (δ , ppm): 195.2, 168.7, 163.1, 157.4, 157.3, 156.5, 150.1, 138.3, 129.3, 128.8,

113.9, 112.1, 96.5, 63.2, 54.3, 54.0, 50.7, 41.1, 33.2, 32.5, 29.4, 27.3, 14.9; HRMS(+ESI) 410.2076 [M + H]⁺.

3.2.11. 5-(3-hydroxyphenyl)-2,4-dimethoxy-8,8-dimethyl-5,8,9,10-tetrahydropyrimido[4,5-*b*]quinolin-6(7*H*)-one (4k). Light brown solid, mp 292–294 °C; ¹H-NMR (500 MHz, CDCl₃ and DMSO-*d*₆) (δ , ppm): 9.73 (s, 1H, NH), 8.89 (s, 1H, OH), 6.95 (t, J = 8 Hz, 1H, ArH), 6.70–6.68 (m, 2H, ArH), 6.53–6.51 (m, 1H, ArH), 5.01 (s, 1H, CH), 3.88 (s, 3H, OCH₃), 3.87 (s, 3H, OCH₃), 2.47 (s, 2H, CH₂), 2.19 (d, J = 16 Hz, 1H, CH₂), 2.10 (d, J = 16 Hz, 1H, CH₂), 1.07 (s, 3H, CH₃), 1.00 (s, 3H, CH₃); ¹³C-NMR (125 MHz, CDCl₃ and DMSO-*d*₆) (δ , ppm): 194.5, 168.4, 163.2, 157.1, 156.8, 151.5, 147.9, 128.8, 118.7, 114.5, 113.2, 110.7, 95.8, 54.5, 53.9, 50.8, 33.8, 32.5, 29.4, 27.4; HRMS(+ESI) 382.1793 [M + H]⁺.

3.2.12. 5-([1,1'-biphenyl]-4-yl)-2,4-dimethoxy-8,8-dimethyl-5,8,9,10-tetrahydropyrimido[4,5-*b*]quinolin-6(7*H*)-one (4l). White solid, mp 246–248 °C; ¹H-NMR (500 MHz, CDCl₃) (δ , ppm): 8.06 (s, 1H, NH), 7.53 (d, J = 7 Hz, 2H, ArH), 7.44 (d, J = 8.5 Hz, 2H, ArH), 7.40–7.37 (m, 4H, ArH), 7.30–7.26 (m, 1H, ArH), 5.25 (s, 1H, CH), 3.920 (s, 3H, OCH₃), 3.915 (s, 3H, OCH₃), 2.47 (s, 2H, CH₂), 2.27 (d, J = 16.5 Hz, 1H, CH₂), 2.22 (d, J = 16.5 Hz, 1H, CH₂), 1.10 (s, 3H, CH₃), 1.03 (s, 3H, CH₃); ¹³C-NMR (125 MHz, CDCl₃) (δ , ppm): 195.1, 168.9, 163.3, 156.4, 150.1, 145.0, 141.1, 139.0, 128.6, 128.4, 127.0, 126.9, 126.8, 112.0, 96.2, 54.5, 54.2, 50.7, 41.3, 33.9, 32.7, 29.4, 27.4; HRMS(+ESI) 442.2121 [M + H]⁺.

3.2.13. 2,4-Dimethoxy-8,8-dimethyl-5-(*p*-tolyl)-5,8,9,10-tetrahydropyrimido[4,5-*b*]quinoline-6(7*H*)-one (4m). White solid, mp 208–210 °C; ¹H-NMR (500 MHz, CDCl₃) (δ , ppm): 8.68 (s, 1H, NH), 7.21 (d, J = 8 Hz, 2H, ArH), 7.01 (d, J = 8 Hz, 2H, ArH), 5.19 (s, 1H, CH), 3.901 (s, 3H, OCH₃), 3.897 (s, 3H, OCH₃), 2.49–2.42 (m, 2H, CH₂), 2.26 (d, J = 14.5 Hz, 1H, CH₂), 2.23 (d, J = 15.5 Hz, 1H, CH₂), 1.08 (s, 3H, CH₃), 1.01 (s, 3H, CH₃); ¹³C-NMR (125 MHz, CDCl₃) (δ , ppm): 195.2, 168.7, 163.1, 156.6, 150.4, 143.1, 135.6, 128.8, 127.7, 112.0, 96.5, 54.3, 54.1, 50.7, 41.1, 33.7, 32.6, 29.5, 27.4, 21.2; HRMS(+ESI) 380.1969 [M + H]⁺.

3.2.14. 5-(4-fluorophenyl)-2,4-dimethoxy-8,8-dimethyl-5,8,9,10-tetrahydropyrimido[4,5-*b*]quinolin-6(7*H*)-one (4n). White solid, mp 200–202 °C; ¹H-NMR (500 MHz, CDCl₃) (δ , ppm): 8.47 (s, 1H, NH), 7.29–7.26 (m, 2H, ArH), 6.91–6.86 (m, 2H, ArH), 5.18 (s, 1H, CH), 3.92 (s, 3H, OCH₃), 3.90 (s, 3H, OCH₃), 2.47 (s, 2H, CH₂), 2.26 (d, J = 16 Hz, 1H, CH₂), 2.20 (d, J = 16 Hz, 1H, CH₂), 1.09 (s, 3H, CH₃), 1.00 (s, 3H, CH₃); ¹³C-NMR (125 MHz, CDCl₃) (δ , ppm): 195.1, 168.8, 162.8 (d, J = 127.9 Hz), 160.3, 156.5, 150.2, 141.8 (d, J = 2.9 Hz), 129.3 (d, J = 7.8 Hz), 114.7 (d, J = 21.2 Hz), 111.9, 96.2, 54.4, 54.1, 50.6, 41.2, 33.6, 32.6, 29.4, 27.3; HRMS(+ESI) 384.1719 [M + H]⁺.

3.2.15. 5-(4-bromophenyl)-2,4-dimethoxy-8,8-dimethyl-5,8,9,10-tetrahydropyrimido[4,5-*b*]quinolin-6(7*H*)-one (4o). Light brown solid, mp 214–216 °C; ¹H-NMR (500 MHz, CDCl₃) (δ , ppm): 8.47 (s, 1H, NH), 7.32 (d, J = 8.5 Hz, 2H, ArH), 7.20 (d, J = 7.5 Hz, 2H, ArH), 5.16 (s, 1H, CH), 3.92 (s, 3H, OCH₃), 3.89 (s, 3H, OCH₃), 2.46 (s, 2H, CH₂), 2.26 (d, J = 16.5 Hz, 1H, CH₂), 2.19 (d, J = 16 Hz, 1H, CH₂), 1.09 (s, 3H, CH₃), 1.00 (s, 3H, CH₃); ¹³C-NMR (125 MHz, CDCl₃) (δ , ppm): 195.0, 168.8, 163.4, 156.5, 150.3, 145.0, 131.1, 129.7, 120.0, 111.5, 95.8, 54.4, 54.1, 50.6, 41.2, 33.9, 32.6, 29.4, 27.3; MS(MM-ES + APCI) 442.20 [M – H][–].



3.2.16. 2,4-Dimethoxy-8,8-dimethyl-5-(4-nitrophenyl)-5,8,9,10-tetrahydropyrimido[4,5-*b*]quinolin-6(7*H*)-one (4p). Light yellow solid, mp 234–236 °C; ¹H-NMR (500 MHz, CDCl₃) (δ , ppm): 8.87 (s, 1H, NH), 8.09 (d, J = 8.5 Hz, 2H, ArH), 7.50 (d, J = 8.5 Hz, 2H, ArH), 5.29 (s, 1H, CH), 3.94 (s, 3H, OCH₃), 3.90 (s, 3H, OCH₃), 2.53 (s, 2H, CH₂), 2.28 (d, J = 16 Hz, 1H, CH₂), 2.19 (d, J = 16.5 Hz, 1H, CH₂), 1.11 (s, 3H, CH₃), 1.00 (s, 3H, CH₃); ¹³C-NMR (125 MHz, CDCl₃) (δ , ppm): 195.0, 168.8, 163.6, 156.6, 153.2, 151.1, 146.3, 128.9, 123.4, 110.7, 95.0, 54.6, 54.3, 50.1, 41.1, 34.8, 32.6, 29.4, 27.2; HRMS(+ESI) 411.1660 [M + H]⁺.

3.2.17. 2,4-Dimethoxy-8,8-dimethyl-5-(2-nitrophenyl)-5,8,9,10-tetrahydropyrimido[4,5-*b*]quinolin-6(7*H*)-one (4q). Light yellow solid, mp 270–272 °C; ¹H-NMR (500 MHz, CDCl₃) (δ , ppm): 7.79 (s, 1H, NH), 7.78–7.77 (m, 1H, ArH), 7.43–7.35 (m, 2H, ArH), 7.24–7.22 (m, 1H, ArH), 6.03 (s, 1H, CH), 3.91 (s, 3H, OCH₃), 3.82 (s, 3H, OCH₃), 2.47–2.43 (m, 2H, CH₂), 2.25 (d, J = 16.5 Hz, 1H, CH₂), 2.16 (d, J = 16.5 Hz, 1H, CH₂), 1.10 (s, 3H, CH₃), 1.01 (s, 3H, CH₃); ¹³C-NMR (125 MHz, CDCl₃) (δ , ppm): 194.7, 169.0, 163.6, 156.0, 150.3, 148.8, 140.2, 132.4, 130.8, 126.9, 124.2, 111.3, 95.3, 54.6, 54.2, 50.4, 41.4, 32.6, 30.2, 29.1, 27.6; HRMS(+ESI) 411.1660 [M + H]⁺.

3.2.18. 2,4-Dimethoxy-8,8-dimethyl-5-(2-nitrophenyl)-5,8,9,10-tetrahydropyrimido[4,5-*b*]quinolin-6(7*H*)-one (4r). Off white solid, mp 236–238 °C; ¹H-NMR (500 MHz, CDCl₃) (δ , ppm): 8.38 (s, 1H, NH), 8.13 (s, 1H, ArH), 7.99 (d, J = 8 Hz, 1H, ArH), 7.74 (d, J = 7.5 Hz, 1H, ArH), 7.40 (t, J = 8 Hz, 1H, ArH), 5.30 (s, 1H, CH), 3.94 (s, 3H, OCH₃), 3.90 (s, 3H, OCH₃), 2.52 (s, 2H, CH₂), 2.28 (d, J = 16.5 Hz, 1H, CH₂), 2.19 (d, J = 16.5 Hz, 1H, CH₂), 1.11 (s, 3H, CH₃), 1.02 (s, 3H, CH₃); ¹³C-NMR (125 MHz, CDCl₃) (δ , ppm): 195.0, 168.8, 163.6, 156.3, 150.8, 148.3, 147.9, 134.5, 128.8, 122.8, 121.5, 110.9, 95.2, 54.6, 54.3, 50.5, 41.2, 34.6, 32.6, 29.4, 27.3; HRMS(+ESI) 411.1660 [M + H]⁺.

3.2.19. 2,4-Dimethoxy-8,8-dimethyl-5-(naphthalen-1-yl)-5,8,9,10-tetrahydropyrimido[4,5-*b*]quinolin-6(7*H*)-one (4s). Off white solid, mp 180–182 °C; ¹H-NMR (500 MHz, CDCl₃) (δ , ppm): 8.79 (s, 1H, NH), 8.56–8.36 (m, 1H, ArH), 6.73 (d, J = 8.5 Hz, 2H, ArH), 5.15 (s, 1H, CH), 3.97–3.92 (m, 2H, CH₂), 3.91 (s, 3H, OCH₃), 3.89 (s, 3H, OCH₃), 2.46–2.44 (m, 2H, CH₂), 2.27–2.18 (m, 2H, CH₂), 1.35 (t, J = 7 Hz, 3H, CH₃), 1.08 (s, 3H, CH₃), 1.00 (s, 3H, CH₃); ¹³C-NMR (125 MHz, CDCl₃) (δ , ppm): 195.3, 169.0, 163.0, 156.2, 133.4, 131.1, 128.1, 127.0, 126.7, 125.5, 125.3, 125.0, 113.4, 97.5, 54.4, 53.8, 50.5, 41.1, 32.5, 29.7, 29.4, 27.3; HRMS(+ESI) 415.2121 [M + NH₄]⁺ [−H₂O].

3.2.20. 5-(6-bromobenzo[d][1,3]dioxol-5-yl)-2,4-dimethoxy-8,8-dimethyl-5,8,9,10-tetrahydropyrimido[4,5-*b*]quinolin-6(7*H*)-one (4t). White solid, mp 296–298 °C; ¹H-NMR (500 MHz, CDCl₃) (δ , ppm): 7.40 (s, 1H, NH), 6.92 (s, 1H, ArH), 6.75 (s, 1H, ArH), 7.74 (d, J = 7.5 Hz, 1H, ArH), 5.88 (dd, J = 8 Hz, 2H, OCH₂O), 5.43 (s, 1H, CH), 3.91 (s, 3H, OCH₃), 3.87 (s, 3H, OCH₃), 2.45–2.37 (m, 2H, CH₂), 2.24 (d, J = 16.5 Hz, 1H, CH₂), 2.18 (d, J = 16.5 Hz, 1H, CH₂), 1.10 (s, 3H, CH₃), 1.05 (s, 3H, CH₃); ¹³C-NMR (125 MHz, CDCl₃) (δ , ppm): 195.0, 169.1, 163.4, 155.8, 149.6, 147.2, 146.5, 114.0, 112.5, 111.7, 110.4, 101.5, 95.7, 54.5, 53.9, 50.6, 41.5, 35.5, 32.6, 29.1, 27.7; HRMS(+ESI) 488.0807 [M + H]⁺.

3.2.21. 5-(2-Butyl-5-chloro-1H-imidazole-4-yl)-2,4-dimethoxy-8,8-dimethyl-5,8,9,10-tetrahydropyrimido[4,5-*b*]quinolin-6(7*H*)-one (4u). Light brown solid, mp 212–214 °C; ¹H-NMR (500 MHz, CDCl₃) (δ , ppm): 9.91 (s, 1H, NH), 8.00 (s, 1H, NH), 5.22 (s, 1H, CH), 3.94 (s, 3H, OCH₃), 3.90 (s, 3H, OCH₃), 2.58 (td, J = 7.5 Hz, 2H, CH₂), 2.43 (d, J = 16.5 Hz, 1H, CH₂), 2.38 (d, J = 17 Hz, 1H, CH₂), 2.29 (d, J = 16.5 Hz, 1H, CH₂), 2.25 (d, J = 16.5 Hz, 1H, CH₂), 1.64 (quin, J = 7.5 Hz, 2H, CH₂), 1.32 (sextet, J = 7.5 Hz, 2H, CH₂), 1.10 (s, 3H, CH₃), 1.03 (s, 3H, CH₃), 0.90 (t, J = 7.5 Hz, 3H, CH₃); ¹³C-NMR (125 MHz, CDCl₃) (δ , ppm): 196.8, 169.1, 163.7, 156.5, 151.6, 145.3, 126.3, 124.1, 108.7, 91.9, 54.6, 54.3, 50.5, 41.21, 32.7, 30.2, 28.9, 28.3, 27.6, 25.8, 22.3, 13.8; HRMS(+ESI) 446.1946 [M + H]⁺.

3.2.22. 5-(5-Bromothiophen-2-yl)-2,4-dimethoxy-8,8-dimethyl-5,8,9,10-tetrahydropyrimido[4,5-*b*]quinolin-6(7*H*)-one (4v). Off white solid, mp 206–208 °C; ¹H-NMR (500 MHz, CDCl₃) (δ , ppm): 8.50 (s, 1H, NH), 6.76 (d, J = 3.5 Hz, 1H, ArH), 6.57 (dd, J = 3.5 Hz, 1H, ArH), 5.49 (s, 1H, CH), 3.98 (s, 3H, OCH₃), 3.94 (s, 3H, OCH₃), 2.48 (d, J = 17 Hz, 1H, CH₂), 2.44 (d, J = 17 Hz, 1H, CH₂), 2.30 (s, 2H, CH₂), 1.11 (s, 3H, CH₃), 1.09 (s, 3H, CH₃); ¹³C-NMR (125 MHz, CDCl₃) (δ , ppm): 195.0, 168.8, 163.4, 156.4, 151.0, 150.8, 129.3, 123.9, 110.6, 109.8, 94.8, 54.5, 54.2, 50.5, 41.1, 32.5, 29.3, 29.3, 27.5; HRMS(+ESI) 451.0624 [M + NH₄]⁺ [−H₂O].

3.3. Antiproliferative activity

The antiproliferative activity was measured using our implementation of the National Cancer Institute (NCI) screening protocol.³⁷ We used the following human solid tumour cell lines: A549 (non-small cell lung), HBL-100 (breast), HeLa (cervix), SW1573 (non-small cell lung), T-47D (breast), and WiDr (colon). Cell seeding densities were 2500 (A549, HBL-100, HeLa, and SW1573) or 5000 (T-47D and WiDr) cells per well. Tested compounds were dissolved in DMSO at an initial concentration of 40 mM. DMSO was used as negative control (0.25% v/v). The results were expressed as GI₅₀, *i.e.* the dose that causes 50% growth inhibition after 48 h of exposure.

3.4. ADMET prediction

In silico ADMET prediction of potent antiproliferative 2,4-dimethoxy-THPQs **4h**, **4o**, **4q** and **4v** were calculated by web tool SwissADME (<http://www.swissadme.ch/>).³⁸

4. Conclusion

In conclusion, we established MWI facilitated green synthetic protocol for a series of 2,4-dimethoxy-THPQs from multicomponent reaction between aldehyde **1**, dimedone **2** and 6-amino-2,4-dimethoxypyrimidine **3** using glacial acetic acid. The main features of this green synthetic protocol are the use of commercially available cheap starting materials, metal-free multicomponent synthesis, short reaction time, higher product yield and no need to column chromatography for product purification. Biological screening showed that the compounds are able to inhibit proliferation of human tumour cells at the micromolar range. The SAR study was not able to



provide information for the future design of new analogues. *In silico* ADMET prediction of antiproliferative 2,4-dimethoxy-THPQs **4h**, **4o**, **4q** and **4v** show good bioavailability radar plot. Furthermore, BOILED-Egg delineation of **4h**, **4o**, **4q** and **4v** show that **4o** have BBB permeability while other show high intestinal absorption. All these also have drug-like properties. Further biological studies will be necessary to identify the cellular targets involved in the biological effects.

Conflicts of interest

The authors declare no conflict of interest.

Acknowledgements

SGP, RMV, PJP and HMP are grateful to the Department of Chemistry, Sardar Patel University for providing lab facilities. SGP is grateful to the UGC, New Delhi for a UGC-JRF (NTA Ref. No.: 201610157514; dated: 01.04.2021). A. G.-B., A. P. and J. M. P. thank the Canary Islands Government (ProID2020010101, ACIISI/FEDER, UE) for financial support. A. P. thanks the EU Social Fund (FSE) and the Canary Islands ACIISI for a predoctoral grant TESIS2020010055. All authors are thankful to Manoj Mangukiya, Associate Analytical Scientist, Aether Industries Ltd, Surat, for the LCMS experiments.

References

- 1 V. A. Katzke, R. Kaaks and T. Kühn, *Cancer J.*, 2015, **21**.
- 2 R. M. Vala, M. G. Sharma, D. M. Patel, A. Puerta, J. M. Padrón, V. Ramkumar, R. L. Gardas and H. M. Patel, *Arch. Pharm.*, 2021, **354**, 2000466.
- 3 D. M. Patel, M. G. Sharma, R. M. Vala, I. Lagunes, A. Puerta, J. M. Padrón, D. P. Rajani and H. M. Patel, *Bioorg. Chem.*, 2019, **86**, 137–150.
- 4 B. Jiang, F. Shi and S.-J. Tu, *Curr. Org. Chem.*, 2010, **14**, 357–378.
- 5 S. Gorle, S. Maddila, S. N. Maddila, K. Naicker, M. Singh, P. Singh and S. B. Jonnalagadda, *Anticancer Agents Med Chem.*, 2017, **17**, 464–470.
- 6 S. Moloi, S. Maddila and S. B. Jonnalagadda, *Res. Chem. Intermed.*, 2017, **43**, 6233–6243.
- 7 E. S. H. El Ashry, E. Ramadan, A. A. Kassem and M. Hagar, *Adv. Heterocycl. Chem.*, 2005, **88**, 1–110.
- 8 Y. Gu, *Green Chem.*, 2012, **14**, 2091–2128.
- 9 S. I. Alqasoumi, A. M. Al-Tawee, A. M. Alafeefy, E. Noaman and M. M. Ghorab, *Eur. J. Med. Chem.*, 2010, **45**, 738–744.
- 10 A. A. Abu-Hashem and A. S. Aly, *Arch. Pharmacal Res.*, 2012, **35**, 437–445.
- 11 M. B. El-Ashmawy, M. A. El-Sherbeny and N. S. El-Gohary, *Med. Chem. Res.*, 2013, **22**, 2724–2736.
- 12 M. M. Ghorab, F. A. Ragab, H. I. Heiba and W. M. Ghorab, *J. Heterocycl. Chem.*, 2011, **48**, 1269–1279.
- 13 R. A. Mekheimer, S. M. R. Allam, M. A. Al-Sheikh, M. S. Moustafa, S. M. Al-Mousawi, Y. A. Mostafa, B. G. M. Youssif, H. A. M. Gomaa, A. M. Hayallah, M. Abdelaziz and K. U. Sadek, *Bioorg. Chem.*, 2022, **121**, 105693.
- 14 M. R. Selim, M. A. Zahran, A. Belal, M. S. Abusaif, S. A. Shedd, A. B. M. Mehany, G. A. M. Elhagali and Y. A. Ammar, *Anti-Cancer Agents Med. Chem.*, 2019, **19**, 439–452.
- 15 E. Tieger, V. Kiss, G. Pokol, Z. Finta, J. Rohlíček, E. Skořepová and M. Dušek, *CrystEngComm*, 2016, **18**, 9260–9274.
- 16 S. Bedi, S. A. Khan, M. M. AbuKhader, P. Alam, N. A. Siddiqui and A. Husain, *Saudi Pharm. J.*, 2018, **26**, 755–763.
- 17 J. Wan, Y. Qiao, X. Chen, J. Wu, L. Zhou, J. Zhang, S. Fang and H. Wang, *Adv. Funct. Mater.*, 2018, **28**, 1804229.
- 18 K. Montazeri and J. Bellmunt, *Expert Rev. Clin. Pharmacol.*, 2020, **13**, 1–6.
- 19 A. Markham, *Drugs*, 2020, **80**, 1345–1353.
- 20 A. K. Larsen, C. M. Galmarini and M. D'Incalci, *Cancer Chemother. Pharmacol.*, 2016, **77**, 663–671.
- 21 S. G. Patel, R. M. Vala, P. J. Patel, D. B. Upadhyay, V. Ramkumar, R. L. Gardas and H. M. Patel, *RSC Adv.*, 2022, **12**, 18806–18820.
- 22 A. Sharma, P. Appukuttan and E. Van der Eycken, *Chem. Commun.*, 2012, **48**, 1623–1637.
- 23 H. R. Prakash Naik, H. S. Bhojya Naik, T. R. Ravikumar Naik, H. R. Naik, D. S. Lamani and T. Aravinda, *J. Sulfur Chem.*, 2008, **29**, 583–592.
- 24 J. Quiroga, J. Trilleras, B. Insuasty, R. Abónia, M. Nogueras, A. Marchal and J. Cobo, *Tetrahedron Lett.*, 2010, **51**, 1107–1109.
- 25 M. H. Mosslemin, E. Zarenehzad, N. Shams, M. N. S. Rad, H. Anaraki-Ardakani and R. Fayazipoor, *J. Chem. Res.*, 2014, **38**, 169–171.
- 26 V. Tandon, R. M. Vala, A. Chen, R. L. Sah, H. M. Patel, M. C. Pirrung and S. Banerjee, *Biosci. Rep.*, 2022, **42**, BSR20212721.
- 27 M. G. Sharma, J. Pandya, D. M. Patel, R. M. Vala, V. Ramkumar, R. Subramanian, V. K. Gupta, R. L. Gardas, A. Dhanasekaran and H. M. Patel, *Polycyclic Aromat. Compd.*, 2021, **41**, 1495–1505.
- 28 H. M. Patel, D. P. Rajani, M. G. Sharma and H. G. Bhatt, *Lett. Drug Des. Discovery*, 2019, **16**, 119–126.
- 29 D. M. Patel, R. M. Vala, M. G. Sharma, D. P. Rajani and H. M. Patel, *ChemistrySelect*, 2019, **4**, 1031–1041.
- 30 H. M. Patel, *Curr. Bioact. Compd.*, 2018, **14**, 278–288.
- 31 M. G. Sharma, R. M. Vala, D. M. Patel, I. Lagunes, M. X. Fernandes, J. M. Padrón, V. Ramkumar, R. L. Gardas and H. M. Patel, *ChemistrySelect*, 2018, **3**, 12163–12168.
- 32 H. M. Patel, *Green Sustainable Chem.*, 2015, **5**, 137.
- 33 D. M. Patel, R. M. Vala, M. G. Sharma, D. P. Rajani and H. M. Patel, *ChemistrySelect*, 2019, **4**, 1031–1041.
- 34 J. Jin, J. Zhang, F. Liu, W. Shang, Y. Xin and S. Zhu, *Chin. J. Chem.*, 2010, **28**, 1217–1222.
- 35 J. A. Mokariya, A. G. Kalola, P. Prasad and M. P. Patel, *Mol. Diversity*, 2022, **26**, 963–979.
- 36 A. Daina and V. Zoete, *ChemMedChem*, 2016, **11**, 1117–1121.
- 37 I. Lagunes, E. Martín-Batista, G. Silveira-Dorta, M. X. Fernandes and J. M. Padrón, *J. Mol. Clin. Med.*, 2018, **1**, 77–84.
- 38 A. Daina, O. Michielin and V. Zoete, *Sci. Rep.*, 2017, **7**, 42717.

